CHINESE OPTICS LETTERS

Vol. 20, No. 7 | July 2022

# Underwater Bessel-like beams with enlarged depth of focus based on fiber microaxicon

Xiaoying He (何晓颖)*, Mengyuan Li (李梦媛), and Lan Rao (饶 岚)**

School of Electronic Engineering, Beijing Key Laboratory of Space-Ground Interconnection and Convergence, and State Key Laboratory of Information Photonics and Optical Communications, Beijing University of Posts and Telecommunications, Beijing 100876, China

*Corresponding author: xiaoyinghe@bupt.edu.cn

**Corresponding author: raolan@bupt.edu.cn

Received February 13, 2022 | Accepted April 8, 2022 | Posted Online May 7, 2022

Underwater optical wireless communication, which is useful for oceanography, environmental monitoring, and underwater surveillance, suffers the limit of the absorption attenuation and Mie–Rayleigh scattering of the lights. Here, Bessel-like beams generated by a fiber microaxicon is utilized for underwater wireless propagation. Underwater, the cone angle for generating Bessel-like beams starts from 46°, which is smaller than that in air for Bessel-like beams. When the cone angle of the fiber microaxicons is about 140°, the depth of focus underwater, which is four times as long as the depth of focus in air, has enlarged about 28 μm, 36.12 μm, and 50.7 μm for 470 nm, 520 nm, and 632 nm visible lights. The transmission distance of the Bessel beams for visible lights has been simulated by using Henyey–Greenstein–Rayleigh phase function methods and spectral absorption by bio-optical model due to Monte Carlo methods. The results show that the propagation distance could reach 4000 m, which overcome the limit of the Mie–Rayleigh scattering and absorption attenuation underwater.

**Keywords:** Bessel-like beams; depth of focus; underwater optical wireless communication.

**DOI:** 10.3788/COL202220.072601

## 1. Introduction

Recently, Bessel-like beams generated by the optical fibers-based method are desirable, which is because they could offer a compact, robust, and alignment-free operation compared with bulky optical systems. So far, there are many fiber-based methods for generating Bessel-like beams, such as fiber microaxicons[1–3], self-growing micro-tips[4], or a tapered hollow tube[5]. Another way is utilizing a long-period grating to excite higher-order cladding mode and then generate Bessel beams with controllable diffraction-resistant distance[6]. These non-diffracting Bessel-like beams have attracted increasing interest owing to their unique light intensity distributions and self-healing propagation properties, which have been widely used in various domains such as optical trapping[7] and manipulation[8], high-order harmonic generation[9], nonlinear optics[10], and material processing[11]. Especially, such properties can also be used in optical wireless communication to overcome the diffraction limits and particle scattering[12], even if encountering opaque obstacles.

As we all know, underwater optical wireless communication is very useful for many applications such as oceanography, environmental monitoring, and underwater surveillance[13,14]. However, it suffers from extreme absorption and Mie–Rayleigh scattering in the water or seawater. Blue–green wavelengths as a distinct transmission window of the seawater for underwater optical wireless communication also suffer the Mie–Rayleigh scattering from water molecules, salt ions, phytoplankton, and other transparent biological organisms[15,16]. Blue–green Bessel-like beams as communication lights underwater could provide a method to solve the problem caused by the Mie–Rayleigh scattering underwater[17].

In this paper, we aim to design fiber microaxicons or microtips and simulate for generating visible Bessel-like beams with long depth of focus (DOF) underwater. It can be utilized in underwater optical wireless communication for long-distance communication, for overcoming such Mie–Rayleigh scattering effects.

## 2. Bessel-like Beam and Its Generation Based on Fiber Microaxicons

An ideal Bessel beam of the $n$th order can be represented by

$$E(r, \phi, z) = A_0 \exp(ik_z z) J_n(k_r r) \exp(\pm in\phi), \quad (1)$$

where $k_r$ is the radial wave vector, $k_z$ is the longitudinal wave vector, $r$ is the radial coordinate, and $r^2 = x^2 + y^2$.

For $n = 0$, which is the zeroth-order Bessel beam that can be easily written through substituting zero for $n$ in Eq. (1), then,

$$E(r, \phi, z) = A_0 \exp(ik_z z) J_0(k_r r). \tag{2}$$

The power contained in the Bessel beam up to radius $b$ is found by integrating Eq. (2):

$$P = A_0^2 \int_0^{2\pi} \int_0^b J_0(k_r r) = A_0^2 B_w^2 \pi [J_0(k_r b)^2 + J_1(k_r b)^2]. \tag{3}$$

As for the optical profile of generated Bessel beams over propagation, the beam envelope propagation method (BPM) is adopted to calculate the Bessel-like beam generation and propagation.

Here, the fiber microaxicon generated by the single mode fiber (SMF) is utilized to generate the Bessel-like beams. The BPM is employed to numerically calculate the intensity distribution in the $x$–$z$ plane for Bessel-like beam generation and propagation. That is because the SMF for the fiber microaxicon is a rotational symmetric structure.

Figure 1(b) shows that the parallel lights from the fiber produce refraction in the microaxicons interface between the fiber and the medium. As we all know, when the refraction angle can reach 90°, the refraction lights into the medium could traverse along the surface of the fiber microaxicon and then disappear, thus being unable to form the Bessel-like beams. The smallest cone angle $\theta$ can be defined by the equation in Fig. 1(b), which comes from the refraction theorem.

For calculations, our designed fiber microaxicon assumed to be axially symmetric with respect to the optical fiber core is shown in Fig. 1, which has large cone angle $\theta$, fiber core diameter of 8 μm, and fiber cladding diameter of 125 μm. Such a fiber microaxicon could be fabricated by a polishing procedure[2]. A visible light source provides the optical mode excitation regime in this fiber microaxicon. The longitudinal ($x$–$z$) power distributions of visible light laser radiation calculated for different cone angles $\theta$ are simulated by BPM. Figure 2 shows that visible light Bessel-like beams of 470 nm, 520 nm, and 632 nm are from fiber microaxicons with different cone angles $\theta$ of 80°, 100°, 120°, 140° and propagated in the air. It can be found that the DOF of Bessel-like beams is dependent on the incident wavelength and cone angle $\theta$. With the increase of the cone angles from 100° to 140°, the DOF of the Bessel-like beam at a wavelength of 470 nm is increased from ~3.8 μm to ~12 μm. With the increase of the incident wavelength from 470 nm to 632 nm, the DOF of the fiber microaxicon with the cone angle of 140° is also increased from ~12 μm to ~14.21 μm. In a word, the large cone angle incident light with long wavelength could lead to large DOF of the fiber microaxicon. The longitudinal ($x$–$z$) power distributions of the Bessel-like beams underwater have been shown in Fig. 3. Comparing Fig. 3 to Fig. 2, it can be found that the underwater Bessel-like beams are easy to generate

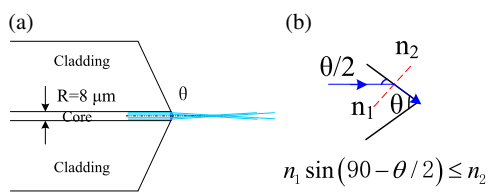


**Fig. 1.** (a) Schematic diagram of the fiber microaxicon, (b) formation principle of the refraction angle for the fiber microaxicon.

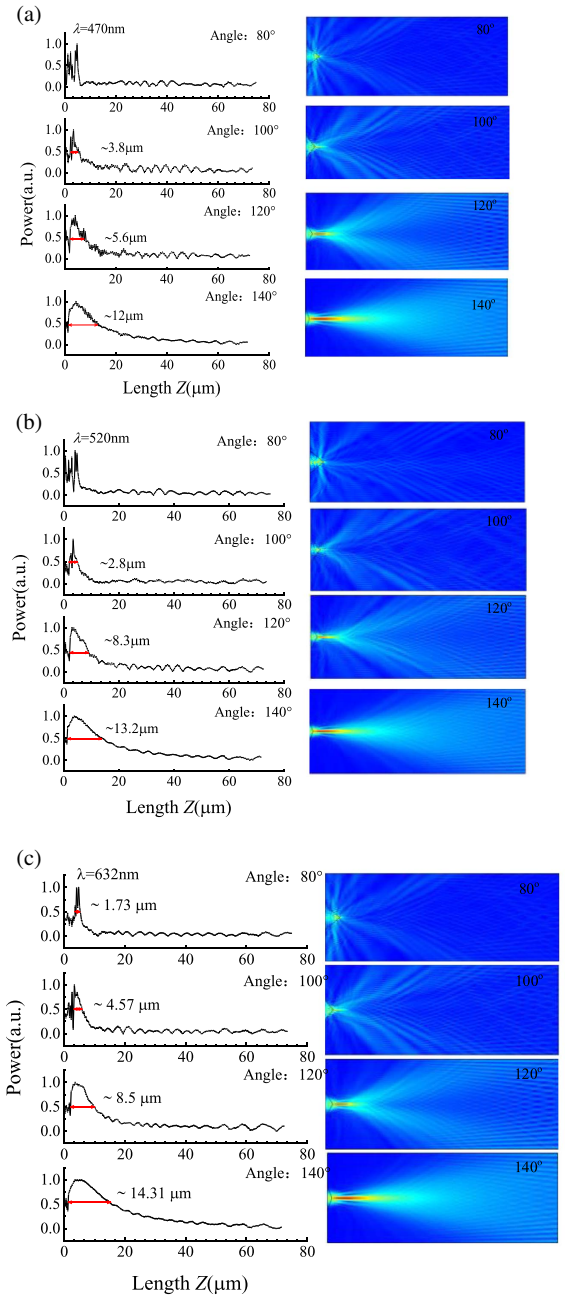


**Fig. 2.** Power distribution of Bessel-like beams from fiber microaxicons with different cone angles of 80°, 100°, 120°, and 140° at different visible wavelengths of (a) 470 nm, (b) 520 nm, and (c) 632 nm in the air.

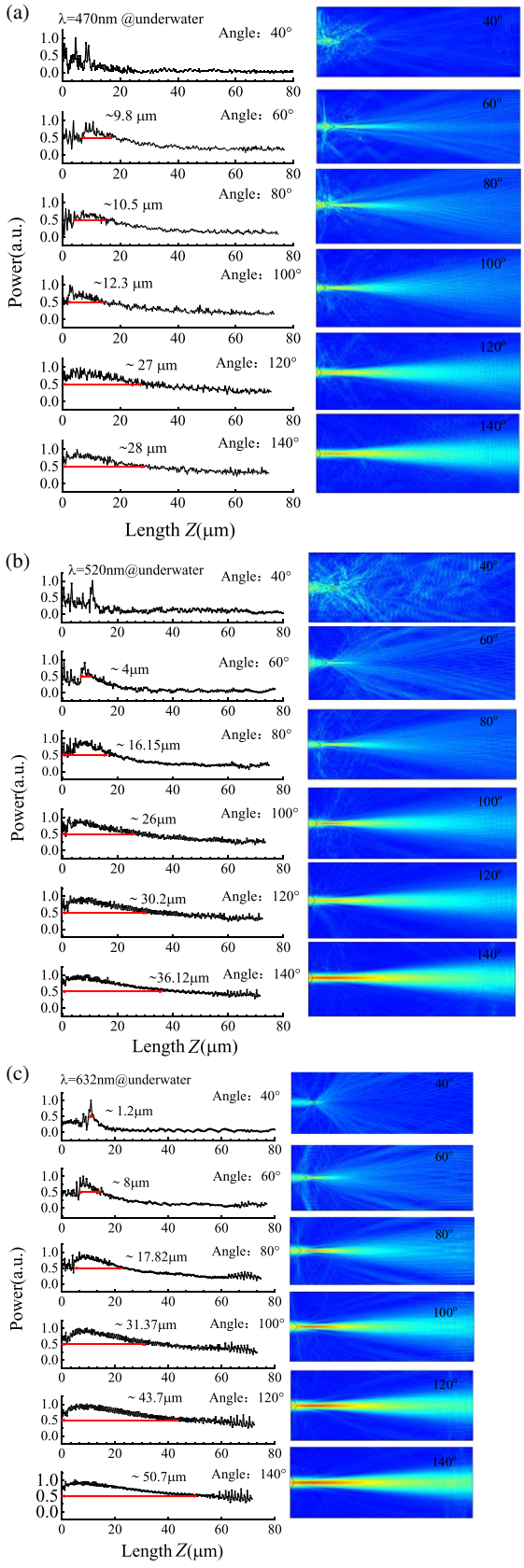


**Fig. 3.** Power distribution of Bessel-like beams underwater from fiber microaxicons with different cone angles of 40°, 60°, 80°, 100°, 120°, and 140° at different wavelengths of (a) 470 nm, (b) 520 nm, and (c) 632 nm.

by using the fiber microaxicon with small cone angles. With the incident light with the wavelength of 470 nm, the fiber microaxicon with the cone angle of 60° could generate the Bessel-like beam underwater, while in the air the fiber microaxicon generating the Bessel-like beam needs the cone angle at about 100°. Thus, the Bessel-like beams in the visible light band have long DOF underwater. When the incident wavelength is changed from 470 to 632 nm at the fiber microaxicon with the cone angle of 140°, its underwater DOF is changed from ~28 μm to ~50.7 μm.

As we all know, the refractive index of water is about 1.33, which is larger than that of the air. According to the equation in Fig. 1(b), the cone angle $\theta$ underwater could be low to that of smaller than the cone angle in the air. According to the calculation, the smallest cone angle $\theta$ of the fiber microaxicon underwater could be as large as 46°, and the smallest cone angle $\theta$ of the fiber microaxicon in the air could reach 95°. These smallest cone angles are close to the simulation results in Figs. 2 and 3.

Figure 4 demonstrates the results in the air and water of numerical calculations of the normalized full width at half-maximum (FWHM) and DOF values as functions of the fiber microaxicons cone angle $\theta$. As shown in Fig. 4(a), in the air, the smallest focal spot with FWHM about ~100 nm, ~220 nm, and ~380 nm, respectively, for wavelengths of 470 nm, 520 nm, and 632 nm is close to the diffraction limit size and can be achieved using fiber microaxicons with the cone angle of 100° for the wavelengths of 470 and 520 nm and the cone angle

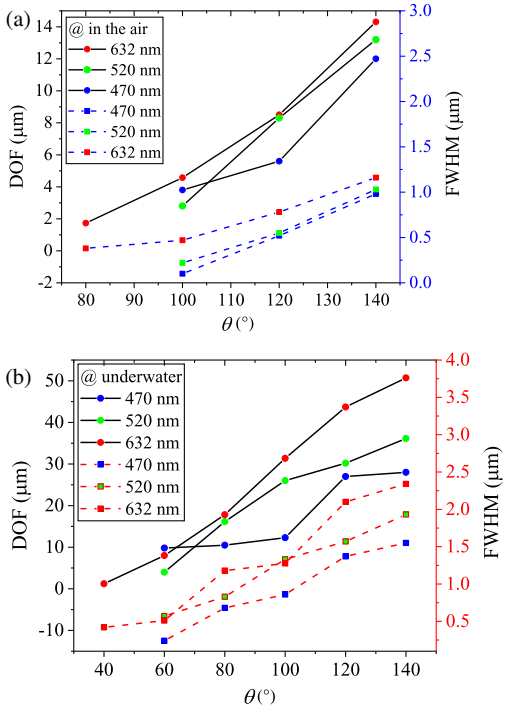


**Fig. 4.** Normalized FWHM and DOF as functions of fiber microaxicons cone angle $\theta$. The solid black lines represent the value of DOF, and the dotted lines represent the value of FWHM. (a) Bessel-like beams generated in the air; (b) Bessel-like beams generated underwater.

of 80° for the 632 nm wavelength. This indicates that the Bessel beam for the short wavelength light has the smallest focal spot with FWHM 100 nm value under the same cone angle. In Fig. 4(b), underwater the smallest focal spot with FWHM ~240 nm, ~570 nm, and ~420 nm, respectively, for wavelengths of 470 nm, 520 nm, and 632 nm, which are all close to their wavelengths and over the diffraction limit size, can be obtained by using the fiber microaxicons with the cone angle of 60° for the wavelengths of 470 and 520 nm and the cone angle of 40° for the 632 nm wavelength. It should be noted that in this case the output beam represents underwater Bessel-like beams with an enlarged DOF, where the DOF value dramatically reaches ~50.7 μm for the 632 nm wavelength, ~36.12 μm for the 520 nm wavelength, and ~28 μm for the 470 nm wavelength at $\theta = 140°$. Summing up these results, for Bessel-like beams with large DOF, fiber microaxicons with $\theta > 140°$ are needed. Thus, for the Bessel-like beams propagated underwater with long distance, $\theta = 140°$ has been chosen.

## 3. Propagation of Bessel-like Beams Underwater

Visible lights indicated into water are attenuated by absorption and scattering. Absorption in water is mainly from an irreversible thermal process whereby the light interacts with water molecules and other organic or non-organic particulates. Scattering in water is described by the process of a photons path changed due to the interaction with particulates in the water. The suspended particles in water such as phytoplankton or other transparent biological organisms are larger than the wavelength of visible lights, which cause Mie scattering. The water molecules and salt ions in water are much smaller than the wavelength of light, which can form Rayleigh scattering. Thus, compared to the effect of scattering, the absorption of the Bessel-like beams underwater for visible lights has a slight effect in this paper. The model of Mie scattering and Rayleigh scattering for Bessel-like beams propagated in water can be established by the Henyey–Greenstein–Rayleigh phase function[18,19], which can be written as

$$P_{\mathrm{HG}}(\theta', g) = \frac{3}{2}\frac{1-g^2}{2+g^2}\frac{1+\cos(\theta')^2}{[1+g^2-2g\cos(\theta')^{3/2}]}, \tag{4}$$

where $g$ is the asymmetry factor, which can be expressed as[18]

$$g = \langle \cos(\theta') \rangle. \tag{5}$$

The Henyey–Greenstein–Rayleigh phase function model can be simulated by using Monte Carlo methods. A pioneering bio-optical model for the spectral absorption coefficient at visible lights was developed by Prieur and Sathyendranath, which can be expressed as[20]

$$\alpha(\lambda) = [\alpha_W(\lambda) + 0.06\alpha_c^*(\lambda)C^{0.65}]\{1 + 0.2\exp[-0.014(\lambda - 440)]\}. \tag{6}$$

Here, $\alpha_W(\lambda)$ is the absorption coefficient of pure water, and $\alpha_c^*(\lambda)$ is a nondimensional, statistically derived chlorophyll-specific absorption coefficient. The $C$ is the chlorophyll concentration. The value of $\alpha_W(\lambda)$ and $\alpha_c^*(\lambda)$ can be obtained from Ref. [20]. From Fig. 3, it is known that the Bessel-like beams generated by the fiber microaxicon have a long DOF underwater, and thus it is suitable for propagation underwater. Lights propagated underwater could suffer from spectral absorption, Mie scattering, and Rayleigh scattering. In this paper, the underwater propagation proceeding of Bessel-like beams generated by the fiber microaxicons has been simulated by using the Henyey–Greenstein–Rayleigh phase function and spectral absorption by a bio-optical model due to Monte Carlo methods. The transverse power distributions of Bessel-like beams generated by the fiber microaxicon with $\theta = 140°$ for three propagation distances of 500 m, 2000 m, and 4000 m are shown in Fig. 5 for visible lights of 470, 520, and 632 nm. It can be shown that the propagation distance is enlarged to 4000 m underwater by Bessel-like beams. It is found in this case that the Bessel-like beams with blue light have a better transmission characteristic than other Bessel-like beams with the green and red lights. This is because the absorption and divergence angle of the blue light are smaller than those of other visible lights. The smallest divergence angle of the central focal spot for the blue light came from the smallest FWHM of the blue Bessel-like mode light generated by the fiber microaxicon with $\theta = 140°$. Underwater, the Bessel-like beams could transmit at least 4000 m. With the increase of the propagation distance, the central focal spot of Bessel-like beams for red light was broadened to be larger than that of blue and green lights. Especially, the Bessel-like beams with the red light transmitted underwater have larger absorption and scattering, and thus its

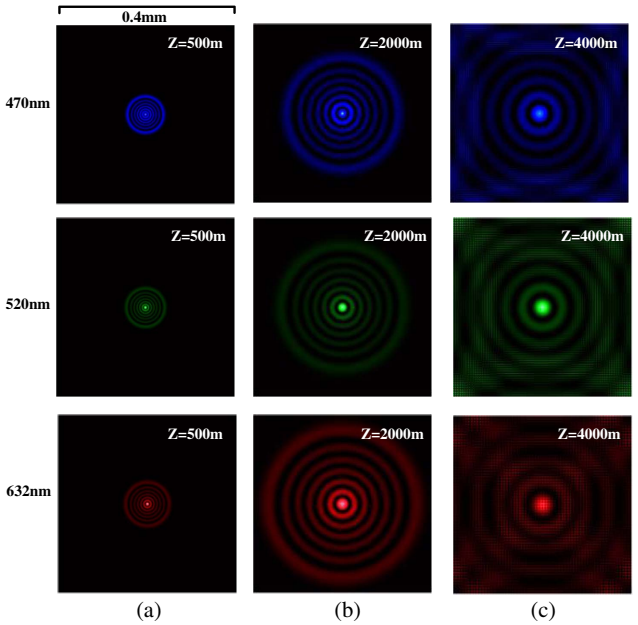


**Fig. 5.** Transverse power distributions of Bessel-like beams with the blue (470 nm), green (520 nm), and red (632 nm) lights generated by the fiber microaxicons underwater for propagation at (a) 500 m, (b) 2000 m, and (c) 4000 m.

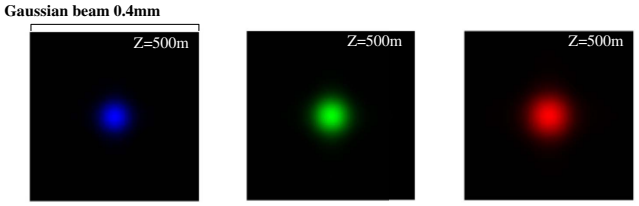


**Fig. 6.** Transverse power distributions of Gaussian beams with the blue (470 nm), green (520 nm), and red (632 nm) lights generated by the fiber microaxicons underwater for propagation at 500 m.

transmission length is no longer than 4000 m. In a word, the blue–green Bessel-like beams are more suitable for underwater communication than the Bessel-like beams with the red light. Figure 6 shows the transverse power distributions of Gaussian beams for the propagation distance of 500 m. Comparing Figs. 5 and 6, under the same propagation distance of 500 m, the light spots expansion of Bessel-like beams caused by the Mie–Rayleigh scattering is smaller than that of Gaussian beams. The transverse power distributions of Bessel-like beams are clearer and smaller than that of Gaussian beams. Thus, it means that Bessel-like beams are more suitable for underwater optical wireless communication.

## 4. Conclusion

Bessel-like beams have been generated by fiber microaxicons with large cone angles in the air and small cone angles in water. Underwater, the cone angle of the fiber microaxicons could be as small as 60° for generating Bessel-like beams for blue light. The Bessel-like beams propagated underwater from the fiber microaxicons with 140° large cone angle have enhanced DOF about 28 μm, 36.12 μm, and 50.7 μm for 470 nm, 520 nm, and 632 nm lights. The enhanced DOF of visible Bessel-like beams generated by fiber microaxicons with cone angle $\theta$ of 140° could improve the propagation distance underwater, which has been simulated to solve the problem of the propagation distance of 1000 m for underwater optical communication. Especially, the Bessel-like beams with blue–green lights could have better focal spots than that of the red light, due to their Bessel-like beams with lower optical absorption and scattering and small divergence angle.

## Acknowledgement

This work was supported by the National Natural Science Foundation of China (Nos. 61675046 and 61604015) and the Fundamental Research Funds for the Central Universities (No. 2021RC05).

## References

1. A. Kuchmizhak, S. Gurbatov, A. Nepomiaschii, O. Vitrik, and Y. Kulchin, "High-quality fiber microaxicons fabricated by a modified chemical etching method for laser focusing and generation of Bessel-like beams," Appl. Opt. **53**, 937 (2014).
2. T. Grosjean, S. S. Saleh, M. A. Suarez, I. A. Ibrahim, V. Piquerey, D. Charraut, and P. Sandoz, "Fiber microaxicons fabricated by a polishing technique for the generation of Bessel-like beams," Appl. Opt. **46**, 8061 (2007).
3. S. Cabrini, C. Liberale, D. Cojoc, A. Carpentiero, M. Prasciolu, S. Mora, V. Degiorgio, F. De Angelis, and E. D. Fabrizio, "Axicon lens on optical fiber forming optical tweezers, made by focused ion beam milling," Microelectron. Eng. **83**, 804 (2006).
4. J. Tan, R. Yu, and L. Xiao, "Bessel-like beams generated via fiber-based polymer microtips," Opt. Lett. **44**, 1007 (2019).
5. C. Chen, Y. Lee, C. Chien, M. Chung, Y. Yu, T. Chen, and C. Lee, "Generating a sub-wavelength Bessel-like light beam using a tapered hollow tube," Opt. Lett. **37**, 4537 (2012).
6. P. Steinvurzel, K. Tantiwanichapan, M. Goto, and S. Ramachandran, "Fiber-based Bessel beams with controllable diffraction-resistant distance," Opt. Lett. **36**, 4671 (2011).
7. S. R. Lee, J. Kim, S. Lee, Y. Jung, J. K. Kim, and K. Oh, "All-silica fiber Bessel-like beam generator and its applications in longitudinal optical trapping and transport of multiple dielectric particles," Opt. Express **18**, 25298 (2010).
8. J. Arlt, V. Garces-Chavez, W. Sibbett, and K. Dholakia, "Optical micromanipulation using a Bessel light beam," Opt. Commun. **197**, 239 (2001).
9. A. Piskarskas, V. Smilgevicius, V. Jarutis, V. Pasiskevicius, S. Wang, J. Tellefsen, and F. Laurell, "Noncollinear second harmonic generation in periodically poled $KTiOPO_4$ excited by the Bessel beam," Opt. Lett. **24**, 1053 (1999).
10. T. Wulle and S. Herminghaus, "Nonlinear optics of Bessel beams," Phys. Rev. Lett. **70**, 1401 (1993).
11. A. Marcinkevicius, S. Juodkazis, S. Matsuo, V. Mizeikis, and H. Misawa, "Application of Bessel beams for microfabrication of dielectrics by femtosecond laser," Jpn. J. Appl. Phys. **40**, L1197 (2001).
12. P. Birch, I. Ituen, R. Young, and C. Chatwin, "Long-distance Bessel beam propagation through Kolmogorov turbulence," J. Opt. Soc. Am. A **32**, 2066 (2015).
13. F. Leccese and G. S. Spagnolo, "State-of-the art and perspectives of underwater optical wireless communications," Acta IMEKO **10**, 25 (2021).
14. G. S. Spagnolo, L. Cozzella, and F. Leccese, "Underwater optical wireless communications: overview," Sensors **20**, 2261 (2020).
15. F. Leccese and G. S. Spagnolo, "LED-to-LED wireless communication between divers," Acta IMEKO **10**, 80 (2021).
16. L. Mullen, "Optical propagation in the underwater environment," Proc. SPIE **7324**, 732409 (2009).
17. Y. Wang, P. Zhang, X. Wang, X. Li, T. Wang, D. Wang, C. Wang, and S. Tong, "Performance analysis in free space underwater data transmission using Bessel–Gaussian beams in a simulated ocean channel with various effects," Opt. Commun. **473**, 125969 (2020).
18. Q. Liu and F. Weng, "Combined Henyey–Greenstein and Rayleigh phase function," Appl. Opt. **45**, 7475 (2006).
19. D. Toublanc, "Henyey–Greenstein and Mie phase functions in Monte Carlo radiative transfer computations," Appl. Opt. **35**, 3270 (1996).
20. C. D. Mobley, *Light and Water: Radiative Transfer in Natural Waters* (Academic Press, 1994).